Stagnation point flow in a vortex core

By L. HATTON, *Department of the Mechanics of Fluids, University of Manchester, England*

(Manuscript received May 15, 1973; revised version September 12, 1974)

ABSTRACT

In an axisymmetric vortex which is in contact with a plane boundary perpendicular to the axis of symmetry, viscous effects will be significant in the vortex core and close to the boundary. Certain types of vortex core have been studied by Rott (1958, 1959) and Bellamy-Knights (1970, 1971), neglecting viscous effects near the boundary. The boundary layer region away from the axis of symmetry has been studied by Bellamy-Knights (1974). On the boundary and near the axis of symmetry, these two viscous regions will interact.

This paper sets out to unify the flows treated by Bellamy-Knights (1971, 1974), by obtaining similarity equations valid in this interaction region, which tend asymptotically to the boundary layer equations with increasing radius and also tend to the core equations with increasing axial distance from the boundary.

An exact solution of the unsteady, viscous, axisymmetric Navier–Stokes equations for an incompressible fluid, relevant to the core and interaction regions, is found as a special case of the solution of the general equations using a certain separation of variables. This reduces the Navier–Stokes equations to two coupled ordinary differential equations which are solved numerically.

The resulting solutions can be used to model the conditions existing at the central core of a tornado vortex. The direction of axial flow in such vortices has long been a matter of some controversy, there being observational evidence for both directions. The solutions described here have the interesting property that either is possible depending on the value of Ω, a parameter proportional to the angular velocity external to the boundary layer. In addition, in some circumstances, the existence of an axial stagnation point aloft is suggested.

1. Introduction

In the past few years, a considerable amount of work has been done in attempting to understand the flow patterns involved in the formation, maintenance and eventual dissolution of tornadoes. Such studies as have been made have led to a dissection of the flow field into four more or less distinct regions (Fig. 1), summarized below. (The mechanics of the region where the funnel meets the cumulo-nimbus cloud structure are largely unknown and will not be considered here.) The extreme violence of the flows involved has meant that there are very few actual measurements of flow parameters and consequently there is still considerable controversy surrounding even the most basic of flow characteristics, for example, whether there is axial upflow or downflow or even both. This particular aspect will receive most attention here. Such uncertainty is due in great part to the difficulties of flow visualization inherent in the problem. For instance, the funnel region, as shown in photographs, is an isobaric surface rather than being directly representative of the velocity field and the debris caught up at the foot of a tornado will not in general follow particle paths.

As a preliminary to the work which follows, the four regions depicted in Fig. 1 will now be discussed briefly. It has been usual to assume axisymmetric flow and so it is convenient to use cylindrical polar coordinates[1] (r, θ, z) where r is the radius, θ the azimuthal angle and z the axial distance from the ground. Region (a), the viscous core region, has been considered by many authors in both steady and unsteady

[1] Serrin (1972), in an individual approach uses spherical polar coordinates with considerable success. He considers a line vortex interacting with a plane boundary, therefore leaving open the problem of the actual structure of the core.

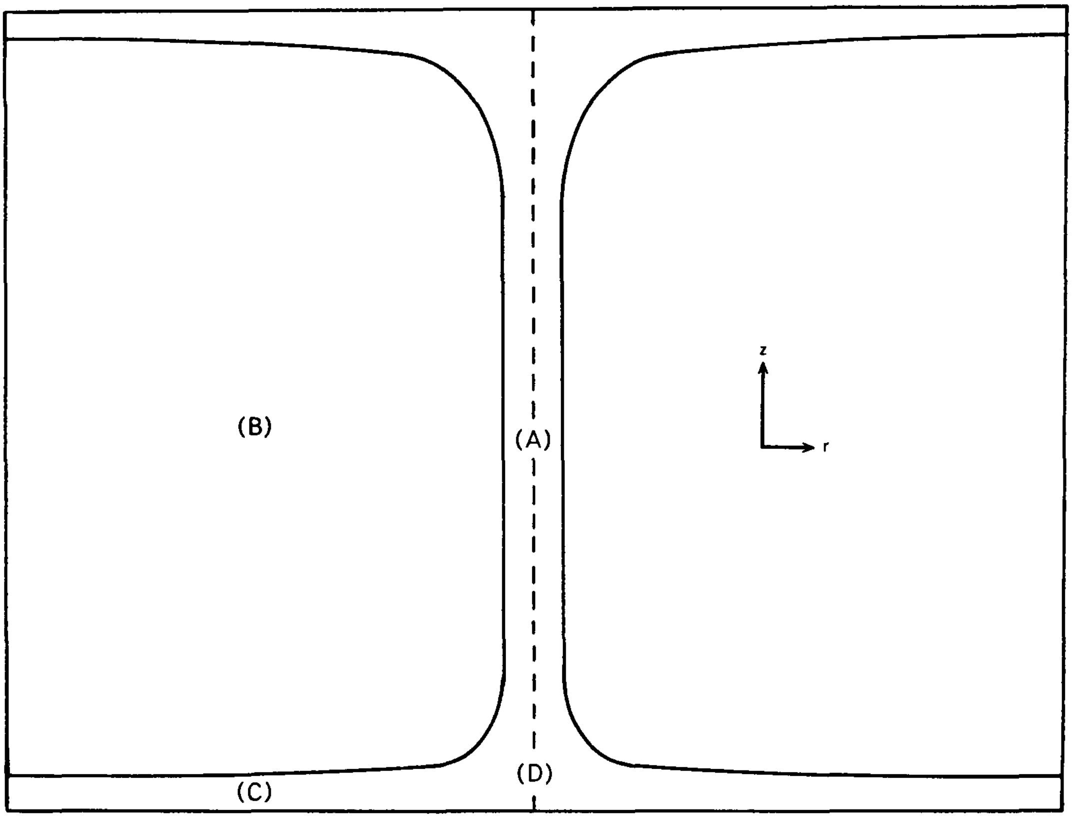

Fig. 1. Diagram of the flow field showing (*a*) the viscous core, (*b*) the outer potential flow, (*c*) the boundary-layer away from the core, and (*d*) the interaction region.

situations. Steady core solutions have been given by Burgers (1940, 1948) and Sullivan (1959), in which the reduction in circumferential velocity at any radius due to the diffusion of the vorticity is balanced by the circumferential velocity increase resulting from the inwards convection of fluid with higher angular momentum. When the radial inflow is insufficient to contain this outward viscous diffusion, the situation is palpably unsteady. Such flows have been considered by Oseen (1911), Rott (1958, 1959) and Bellamy-Knights (1970, 1971). In particular, Oseen and Bellamy-Knights consider a similarity analysis in terms of the variable $\eta = r^2/4\nu t$, where ν is the kinematic viscosity and t represents time. A feature common to all these solutions is a velocity field (u, v, w), in cylindrical polar coordinates, of the form

$$u = u(r, t) \quad v = v(r, t) \quad w = z\bar{w}(r, t) \qquad (1)$$

The limitations of such solutions will be discussed below.

Region (*b*) is a potential flow region well away from the effects of both the plane boundary and the vortex core. This provides the outer boundary conditions for both the core region and the boundary layer region (*c*), discussed later. In the work of Bellamy-Knights, this outer flow is assumed to be

$$u = -\frac{\gamma r}{2t} \quad v = \frac{K_c}{r} \quad w = \frac{\gamma z}{t}$$

where γ is a parameter governing the radial flow and $2\pi K_c$ is the circulation.

The third region, the boundary layer away from the core ((*c*), Fig. 1), has been considered by, for example, Bellamy-Knights (1974). His approach is based on a similarity analysis using the boundary layer variable $\xi = z/2\sqrt{\nu t}$. His work shows that such boundary layers exist provided that the value of γ lies in the same range as his 1971 paper indicated for the existence of his core solutions.

The present work arose from an investigation into the 'stagnation point' region ((*d*), Fig. 1), using a similarity analysis in both of the aforementioned variables η, ξ. The mathematical procedure used is as follows. The complete axisymmetric Navier–Stokes equations for unsteady, viscous, incompressible flow are reduced to two equations for two dependent variables, a stream function ψ and a circulation function $K = rv$, in terms of three independent variables η, ξ and t. A search for solutions in terms of the η, ξ variables alone leaves two equations valid in the stagnation point region.

In section 3, an exact solution for these equations is found by separation of variables which reduces the system to two coupled ordinary differential equations which can, for $\gamma = -1$ only, be solved numerically. This gives a boundary layer solution with an outer potential flow of the form

$$u = \frac{r}{2t} \quad v = \frac{\Omega r}{4t} \quad w = -\frac{z}{t}$$

where $\Omega = K_c/\nu$.

This solution corresponds to a column of fluid in solid body rotation above a plane boundary but shearing in horizontal planes near the boundary in order to satisfy the no-slip condition there. The column also moves towards the boundary, there being a corresponding radial outflow in order that continuity be satisfied.

It has been pointed out by Morton (1972), that vortices with a structure corresponding to (1) are weak vortices in the sense that they are driven by the outer flow and as such may not bear much resemblance to a tornado vortex as they also fail to satisfy the no-slip condition at $z = 0$. The present work seems to suggest that this limitation at the ground can be removed but only for small radius if it is to be relevant to the tornado vortex. Only then can the swirl velocity be assumed proportional to r. Hence, in this case, the no-slip condition is satisfied at the cost of relinquishing the physically more realistic condition of constant circulation away from the core.

On the question of the direction of axial flow, there is evidence for both upflow and downflow near the ground. The existence of downflow is demonstrated rather forcibly by Rossmann (1960), who shows a photograph of pine planks driven half a metre into firm ground after the passage of a tornado core. Gutman (1957) also reports observations that branches, grass and other objects are frequently found as though screwed into the ground in the wake of such a core. On the other hand, Hoecker (1960), analysing the Dallas tornado of the 2nd April 1957, observed a region of *upflow* near the ground terminated by an axial stagnation point aloft and downward flow above that. He notes that more debris may be carried up when a funnel is suspended than when it is at the ground, and that objects carried up under a suspended funnel may hesitate aloft before being ejected outwards, indicating stagnation on the axis. Recent experimental work by Ward (1972) also indicates the existence of both of these flow situations. As will be seen, the present work suggests that these two apparently conflicting flow situations could be reconciled as being simply cases with different Ω resulting in different flow patterns provided that they are fully developed in the sense that there is a central region of solid body rotation throughout the core. It may be noted that this region is not necessarily coincident with the visible funnel.

2. The governing equations

The starting point of the analysis is the full, unsteady, viscous, axisymmetric Navier–Stokes equations, coupled with the continuity equation. For reasons to be discussed later, these will be considered in a laminar, incompressible form without buoyancy contributions. It may also be noted that dynamically allowable solutions are being sought without reference to the energy mechanism supporting them, so the energy equation is not required in this work.

In cylindrical polars, the Navier–Stokes equations then take the form

$$\frac{\partial u}{\partial t} + u\frac{\partial u}{\partial r} + w\frac{\partial u}{\partial z} - \frac{v^2}{r} = -\frac{1}{\varrho}\frac{\partial p}{\partial r} + \nu\left\{\frac{\partial}{\partial r}\left(\frac{1}{r}\frac{\partial}{\partial r}(ru)\right) + \frac{\partial^2 v}{\partial z^2}\right\} \quad (2)$$

$$\frac{\partial v}{\partial t} + u\frac{\partial v}{\partial r} + w\frac{\partial v}{\partial z} + \frac{uv}{r} = \nu\left\{\frac{\partial}{\partial r}\left(\frac{1}{r}\frac{\partial}{\partial r}(rv)\right) + \frac{\partial^2 v}{\partial z^2}\right\} \quad (3)$$

$$\frac{\partial w}{\partial t} + u\frac{\partial w}{\partial r} + w\frac{\partial w}{\partial z} = -\frac{1}{\varrho}\frac{\partial p}{\partial z} + \nu\left\{\frac{1}{r}\frac{\partial}{\partial r}\left(r\frac{\partial w}{\partial r}\right) + \frac{\partial^2 w}{\partial z^2}\right\} \quad (4)$$

where ϱ is the density and p is the pressure.

The continuity equation is

$$\frac{\partial u}{\partial r} + \frac{u}{r} + \frac{\partial w}{\partial z} = 0 \quad (5)$$

These equations may be reduced to a more tractable form by expressing them in terms of two dependent variables, the stream function ψ, replacing the continuity equation, and the circulation function K, where

$$(u, v, w) = \frac{1}{r}\left(-\frac{\partial \psi}{\partial z}, K, \frac{\partial \psi}{\partial r}\right) \quad (6)$$

Eliminating p from (2) and (4) gives

$$-\frac{1}{r}D^2\left(\frac{\partial \psi}{\partial t}\right) + \frac{\partial((1/r^2)D^2\psi, \psi)}{\partial(r, z)} - \frac{1}{r^3}\frac{\partial K^2}{\partial z} = -\frac{\nu}{r}D^4\psi \quad (7)$$

where D^2 is the Stokes operator defined by

$$D^2 = \frac{\partial^2}{\partial r^2} - \frac{1}{r}\frac{\partial}{\partial r} + \frac{\partial}{\partial z^2} \equiv r\frac{\partial}{\partial r}\left(\frac{1}{r}\frac{\partial}{\partial r}\right) + \frac{\partial^2}{\partial z^2}$$

and

$$\frac{\partial(f, g)}{\partial(x, y)} \equiv \left(\frac{\partial f}{\partial x}\right)_y\left(\frac{\partial g}{\partial y}\right)_x - \left(\frac{\partial f}{\partial y}\right)_x\left(\frac{\partial g}{\partial x}\right)_y$$

The various terms in (7) represent, from left to right, an unsteady term, a convective acceleration term, a coupling with the circulation and a viscous term.

The circumferential momentum equation (3) can be written as

$$\frac{\partial K}{\partial t} - \frac{1}{r}\frac{\partial(K, \psi)}{\partial(r, z)} = \nu D^2 K \quad (8)$$

Following Bellamy-Knights (1971, 1974), the similarity variables

$$\eta = \frac{r^2}{4\nu t} \quad \xi = \frac{z}{2\sqrt{\nu t}} \quad (9)$$

are introduced.

Equations (7) and (8) can then be written

$$-D^2(A\psi) + \frac{\eta}{4(\nu t)^{3/2}}\frac{\partial((1/\eta)D^2\psi, \psi)}{\partial(\eta, \xi)} - \frac{1}{8\eta(\nu t)^{3/2}}\frac{\partial K^2}{\partial \xi} = -\nu D^4\psi \quad (10)$$

and

$$AK - \frac{1}{4(\nu t)^{3/2}}\frac{\partial(K, \psi)}{\partial(\eta, \xi)} = \nu D^2 K \quad (11)$$

where

$$D^2 \equiv \frac{1}{\nu t}\left(\eta\frac{\partial^2}{\partial \eta^2} + \frac{1}{4}\frac{\partial^2}{\partial \xi^2}\right)$$

and

$$A \equiv \frac{1}{t}\left(-\eta\frac{\partial}{\partial \eta} - \frac{\xi}{2}\frac{\partial}{\partial \xi} + t\frac{\partial}{\partial t}\right)$$

Solutions are now sought in terms of η, ξ only. Hence, let

$$\frac{\psi}{4\nu\sqrt{\nu t}} = \hat{M}(\eta, \xi)$$

$$\frac{K}{K_c} = \hat{N}(\eta, \xi)$$

where the factor 4 is introduced for convenience and the ^ signifies nondimensional quantities. K_c is a constant with the dimensions of circulation.

Then (10) and (11) become

$$\hat{N}\frac{\partial \hat{N}}{\partial \xi} = 16\frac{\nu^2}{K_c^2}\left\{\eta^2\frac{\partial((1/\eta)B^2\hat{M}, \hat{M})}{\partial(\eta, \xi)} - \eta(B^2(L\hat{M}) - B^4\hat{M})\right\} \quad (12)$$

and

$$B^2\hat{N} + \eta\frac{\partial \hat{N}}{\partial \eta} + \frac{\xi}{2}\frac{\partial \hat{N}}{\partial \xi} = \frac{\partial(\hat{M}, \hat{N})}{\partial \eta\ \xi)} \quad (13)$$

where

$$L(\eta, \xi) \equiv -\eta\frac{\partial}{\partial \eta} - \frac{\xi}{2}\frac{\partial}{\partial \xi} + \frac{1}{2}$$

and

$$B^2(\eta, \xi) \equiv \eta\frac{\partial^2}{\partial \eta^2} + \frac{1}{4}\frac{\partial^2}{\partial \xi^2}$$

In view of the complexity of these equations, a further simplification is sought:

$$\left.\begin{aligned}\hat{M}(\eta,\xi) &= f(\eta)F(\xi)\\ \hat{N}(\eta,\xi) &= h(\eta)H(\xi)\end{aligned}\right\} \qquad (14)$$

Such a separation is suggested by the fact that in the core region (Fig. 1*a*), it was found that $\hat{M}$ and $\hat{N}$ were basically functions of η only (e.g. Bellamy-Knights, 1971), whereas in the boundary layer region (Fig. 1*c*), they were functions of ξ only (Bellamy-Knights, 1974). This is essentially due to the fact that both of these regions exhibit boundary layer type behaviour and therefore derivatives with respect to the length coordinate of the respective boundary layer (e.g. ξ for the core region) are neglected compared with corresponding derivatives with respect to the width coordinate (η for the core region).

Substituting from (14) into the system (12), (13) yields

$$\begin{aligned}h^2HH' = \frac{\nu^2}{K_c^2}&(16\eta^3Ff''' + 8\xi\eta^2f''F' + 4\eta^2f'F''\\ &+ 2\eta\xi fF''' + 24\eta^2f''F + 2\eta fF''\\ &+ 16\eta^2ff'''FF' - 16\eta^2f'f''FF' - 4f^2F'F''\\ &+ 4\eta ff'F'F'' - 4\eta ff'FF''' + 16\eta^3f''''F\\ &+ 8\eta^2f''F'' + \eta fF'''' + 32\eta^2f'''F)\end{aligned} \qquad (15)$$

and

$$\eta\frac{h''}{h} + \frac{1}{4}\frac{H''}{H} + \eta\frac{h'}{h} + \frac{\xi}{2}\frac{H'}{H} = \frac{H'}{H}f'F - \frac{h'}{h}fF' \qquad (16)$$

which represent the complete Navier–Stokes equations for the laminar, axisymmetric flow of an incompressible fluid in the absence of body forces, for the particular separation of variables

$$\left.\begin{aligned}\psi(\eta,\xi,t) &= 4\nu\sqrt{\nu t}\,f(\eta)F(\xi)\\ K(\eta,\xi) &= K_c\,h(\eta)H(\xi)\end{aligned}\right\} \qquad (17)$$

The boundary conditions for the flow are $f(0) = h(0) = 0$ corresponding to zero radial velocity and zero swirl velocity on the axis $r = 0$.

Also $\partial w/\partial r = 0$, giving the extra condition that $f''(0)$ is bounded.

The no-slip condition on the ground $z = 0$ requires

$$F(0) = F'(0) = H(0) = 0 \qquad (18)$$

With reference to Fig. 1, as $\xi \to \infty$ for small η, the core region is entered, in which $F(\xi) = \xi - C$, $H(\xi) = 1$, and C is a constant. Hence, applying the boundary conditions

$$F \to \xi - C, \quad H \to 1 \quad \text{as } \xi \to \infty \qquad (19)$$

the flow becomes the essentially η-dependent core flow mentioned earlier. In this limit (15) and (16), after one integration, reduce to the following equations for the core region, considered by Bellamy-Knights (1971)

$$(\eta f'' + \eta f')' + ff'' - (f')^2 + \text{constant} = 0$$

$$\eta h'' + \eta h' + fh' = 0$$

Similarly, as $\eta \to \infty$ for small ξ, the boundary layer region (Fig. 1*c*) is entered, in which $f(\eta) = \gamma\eta + D$, $h(\eta) = 1$, and D is a constant. Thus applying the boundary conditions

$$f \to \gamma\eta + D, \quad h \to 1 \quad \text{as } \eta \to \infty$$

the ξ-dependent boundary layer region is obtained, and (15) and (16), again after one integration, reduce to

$$F''' + 2\xi F'' + 4F' + 2\gamma((F')^2 - 2FF'') + \text{constant} = 0$$

$$H'' + 2\xi H' - 4\gamma FH' = 0$$

which are the equations derived by Bellamy-Knights (1974) for this region.

3. A particular solution of the governing equations

Ideally, it is required to find a solution for the stagnation point region which asymptotes to a solution for the core region as $\xi \to \infty$, and to a solution for the boundary layer region as $\eta \to \infty$ (see Fig. 1). Although such a solution has not yet been obtained, by confining attention to the core region, the conditions as $\xi \to \infty$ can be satisfied as will now be shown.

The simplest core flow solution is that obtained by Rott and given by

$$f = \gamma\eta$$

and when η is small, $h \propto \eta$, corresponding to rigid body rotation. This suggests that when r is small, the core solution approximates to

$$u = -\frac{\gamma r}{2t} \quad v = \frac{\Omega r}{4t} \quad w = \frac{\gamma z}{t} \tag{20}$$

where $\Omega/4t$ is the angular velocity. This velocity field must satisfy the equations of motion and if the relations (20) are substituted into the circumferential momentum equation (3), it is found that $\gamma = -1$ for all $\Omega \neq 0$.

Adopting this simplification, an example of the use of the general equations is now given in which it is assumed that away from the boundary the core flow consists of a radial flow specified by $f = -\eta$ and an unsteady rigid body rotation, corresponding to $h(\eta) \propto \eta$. One weakness of such a solution is that the circumferential velocity does not tend asymptotically to its value in the boundary layer solution for large r. It may, however, be a reasonable approximation for the core flow for small r.

It is found that for the particular substitution $f = -\eta$, $h = \eta$ (absorbing any other multiplicative constants), the equations (15) and (16), after putting $\gamma = -1$, become

$$F'''' + 2\xi F''' + 4FF''' + 6F'' = -\Omega^2 HH' \tag{21}$$

$$H'' + 2\xi H' + 4H = 4(F'H - FH') \tag{22}$$

Equation (21) can immediately be integrated once to give

$$F''' + 2\xi F'' + 4F' + 4FF'' - 2(F')^2 + \frac{\Omega^2 H^2}{2} = 2 + \frac{\Omega^2}{2} \tag{23}$$

where the constant of integration is obtained by substituting the values of F, H and their derivatives as $\xi \to \infty$, where it is assumed that $\xi F'' \to 0$. This latter assumption is supported by all subsequent numerical calculations.

Summarizing then, the velocity field

$$u = \frac{r}{2t}F'(\xi) \quad v = \frac{\Omega r}{4t}H(\xi) \quad w = -2\sqrt{\frac{\nu}{t}}F(\xi) \tag{24}$$

where $F(\xi)$, $H(\xi)$ satisfy the coupled system (22), (23) subject to the boundary conditions (18) and (19), represents an exact separable solution of the Navier–Stokes equations corresponding to an outer potential flow of type (20) with $\gamma = -1$, satisfying the no-slip condition on a plane, fixed boundary at $z = 0$. It may be noted that the sense of rotation is unimportant as the presence of Ω^2 in (23) means that if Ω is a solution, then $-\Omega$ is also. Furthermore, the case $\Omega = 0$ corresponds to a simple radial-axial flow with no swirl.

Finally, defining the non-dimensional pressure by

$$\hat{p} = \frac{pt}{2\nu\varrho}$$

the pressure field corresponding to (24) is

$$\hat{p} = (4 + \Omega^2)\,\eta - F^2(\xi) - \frac{F'(\xi)}{2} - \xi F(\xi) \tag{25}$$

4. Numerical integration of equations

The coupled ordinary differential equations (22) and (23) subject to the boundary conditions (18) and (19), were solved numerically on an ICL 1906A computer using a library routine for solving the two-point boundary value problem for a system of n ordinary differential equations in a given range $(0, \xi_e)$. ξ_e is chosen sufficiently large so that $\xi_e > \xi_b$, the edge of the boundary layer.

To use the routine, the values of H, H', F, F', and F'' at $\xi = 0$ and $\xi = \xi_e$ must be specified. In this case, seven of these boundary values are known from the no-slip conditions (18) and the conditions at infinity (19). The routine then uses a modified shooting method which starts with approximations to the unknown boundary conditions $H'(0)$, $F''(0)$ and $F(\xi_e)$, and exits with values of these which satisfy the original differential equations (22), (23) and the known boundary conditions (18) and (19), to the desired accuracy.

Computation was started at $\Omega = 0$ (zero-swirl) and increased in increments $\Delta\Omega$. The converged boundary conditions for each value of Ω were used as starting values for the next value, $\Omega + \Delta\Omega$. Although this method relies on the continuous dependence of the solution on parameter values no trouble was encountered.

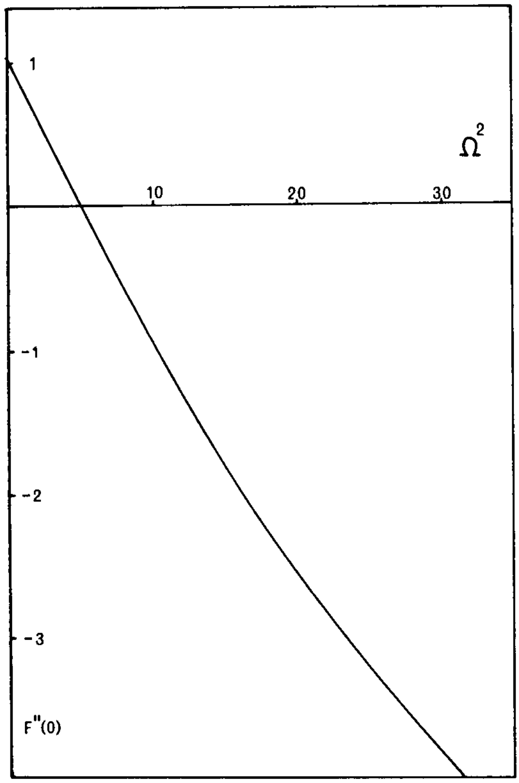

Fig. 2. $F''(0)$ v. Ω^2.

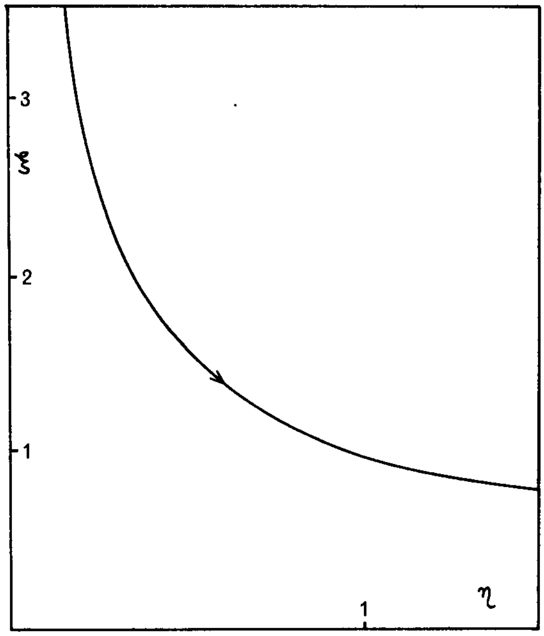

Fig. 3. A typical unseparated streamline.

The program was also run in a more general form in which the parameter Ω could be continuously changed as part of the matching process, giving some insight into the question of uniqueness which will be discussed briefly in the next section. Some programs were run as far as $\xi = 30\ \xi_b$, over which range errors due to discretization and numerical instability were negligible.

5. Discussion of results

The numerical results showed that, for various values of the parameter Ω, solutions of (22) and (23) were found satisfying the boundary conditions (18), (19), provided $\gamma = -1$, giving a radially outward flow outside the boundary layer.

The question of uniqueness, namely whether at most one flow can exist for each value of Ω, has been left open. While this seems likely, and the numerical work supports this conjecture, the complexity of the relevant differential equations makes this, and the question of whether the solutions depend continuously on the parameter Ω, unanswerable at present.

The major part of the discussion will be

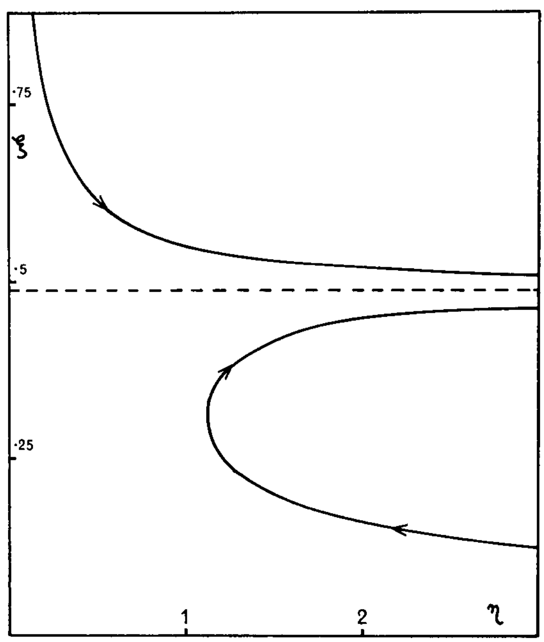

Fig. 4. A typical separated streamline.

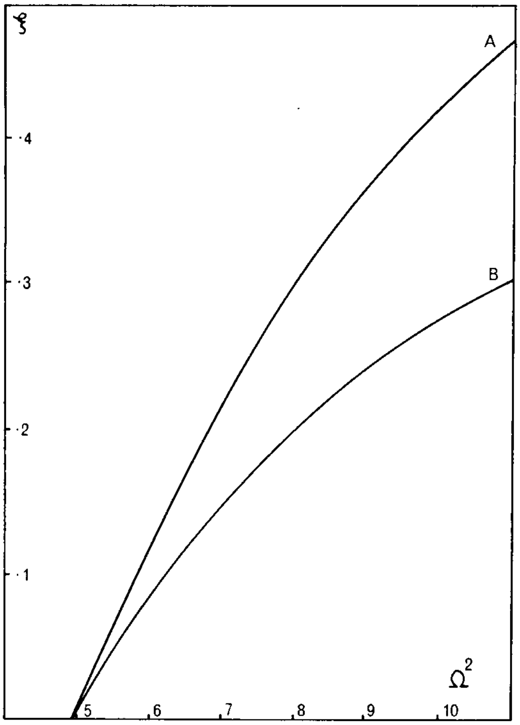

Fig. 5. Curve A shows the variation of the height of the stagnation point with Ω^2. Curve B indicates the height at which the radial velocity is zero.

centred on the two types of flow occurring. These are distinguishable by the sign of $F''(0)$ (essentially $\partial u/\partial z$ on the boundary), and Fig. 2 shows the behaviour of $F''(0)$ as the parameter Ω^2 varies. It may be seen that for $0 \leqslant \Omega^2 \leqslant 4.952 = A$ say, $F''(0) > 0$, whilst for $\Omega^2 > A$, $F''(0) < 0$, giving reversed flow adjacent to the boundary. The flows for Ω^2 less than and greater than A will be referred to as unseparated and separated boundary layer solutions respectively.

An unseparated boundary layer solution has axial downflow for all ξ, i.e. throughout the column. Such a solution is shown in Fig. 3 which gives a typical streamline for a value of $\Omega^2 < A$. When $\Omega^2 > A$, however, $F''(0) < 0$, and there is an axial stagnation point aloft with associated upflow in a cell adjacent to the ground. Fig. 4 illustrates a typical streamline for the case $\Omega^2 = 11.46 > A$, whilst Fig. 5 shows how the height of the stagnation point above the boundary varies with Ω^2.

Figs. 6 and 7 show the variation of the radial velocity F' and the circumferential velocity H respectively, with Ω^2. The development of the radial velocity profiles with Ω^2 is clearly seen here. The circumferential velocity, however, is much less sensitive to such changes in Ω and the variations are not detectable on the scale of this Figure. However, a detailed investigation shows that an

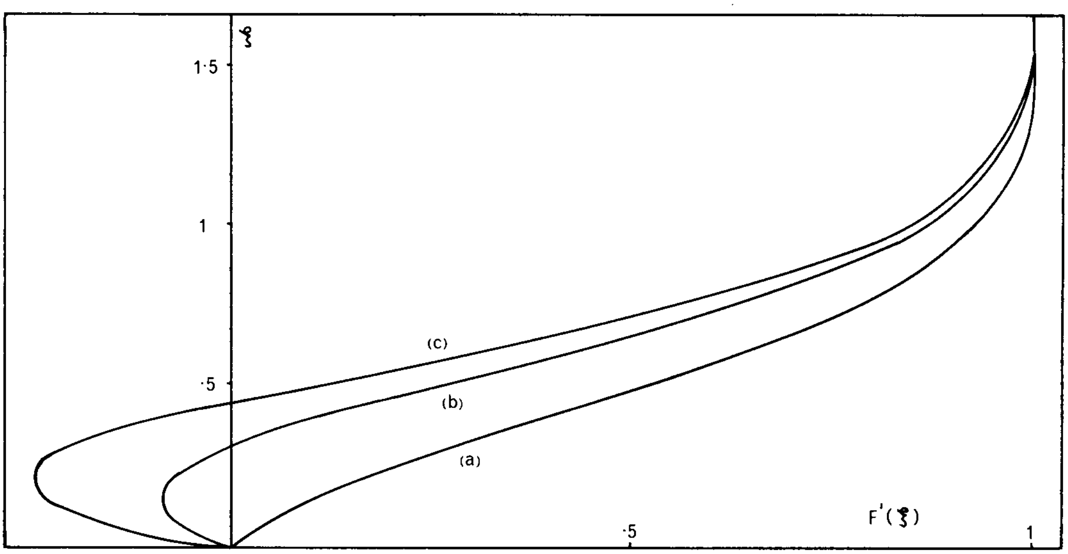

Fig. 6. Radial velocity profiles for $\Omega^2 = 2.6$, 11.46, 20 (curves (a), (b), (c) respectively).

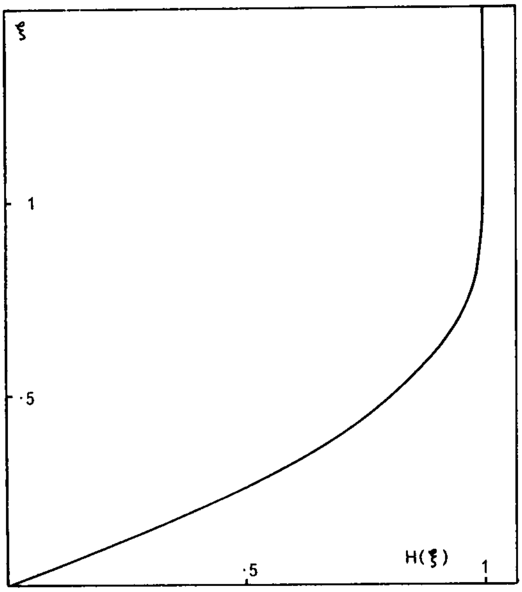

Fig. 7. Tangential velocity profile for values of Ω^2 considered here ($\Omega^2 \leq 30$).

increase in the value of Ω^2 causes $H'(0)$ to increase, i.e. increased angular velocity leads to slightly larger values of H at corresponding values of ξ and this is as expected.

The function F, corresponding to the axial velocity is shown in Fig. 8 for both separated and unseparated solutions. The curve $F = \xi$ is also plotted illustrating the boundary condition $F(\xi) \to \xi - C$ as $\xi \to \infty$. The constant C then represents the horizontal displacement in the lines after they have become parallel at about $\xi = 1.5$.

The physical situation represented by the two kinds of boundary layer solutions discussed above is essentially as follows. Away from the boundary layer, there is a balance between centrifugal and convective acceleration terms and an inward pressure gradient. This balance ceases to be maintained near the boundary because the centrifugal and convective fields are disrupted by the presence of the boundary whereas the inward pressure gradient is much less affected. The unseparated solution then shows an axial downflow and radial outflow decelerated by the presence of the otherwise unbalanced inward pressure gradient. As Ω^2 increases, the radially inward pressure gradient must be correspondingly larger to balance the higher centrifugal acceleration in the core and eventually, in the boundary layer where the centrifugal field is depressed, overcomes the radial outflow thus causing a cell of reversed flow in the neighbourhood of the ground.

Finally, the isobars of the dynamic pressure field $\hat{p}$ are shown in Fig. 9 for both separated and unseparated solutions. It may be noted that in both cases the isobars are funnel-

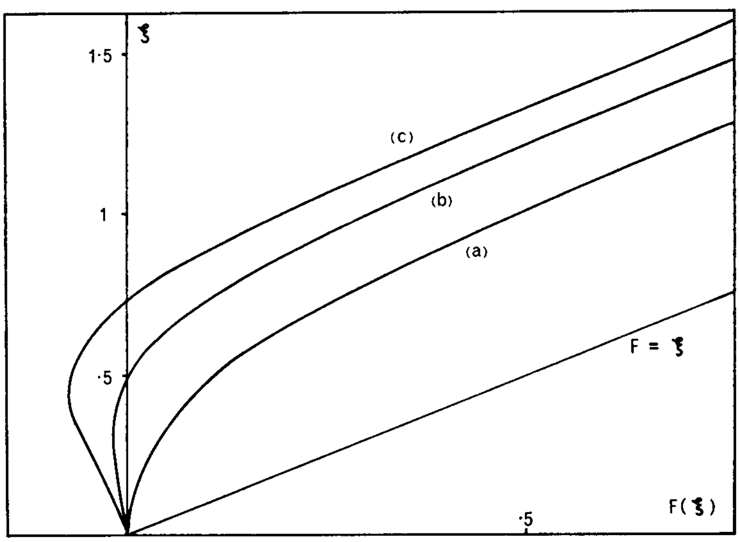

Fig. 8. Axial velocity profiles for $\Omega^2 = 2.6$, 11.46, 20 (curves (*a*), (*b*), (*c*) respectively).

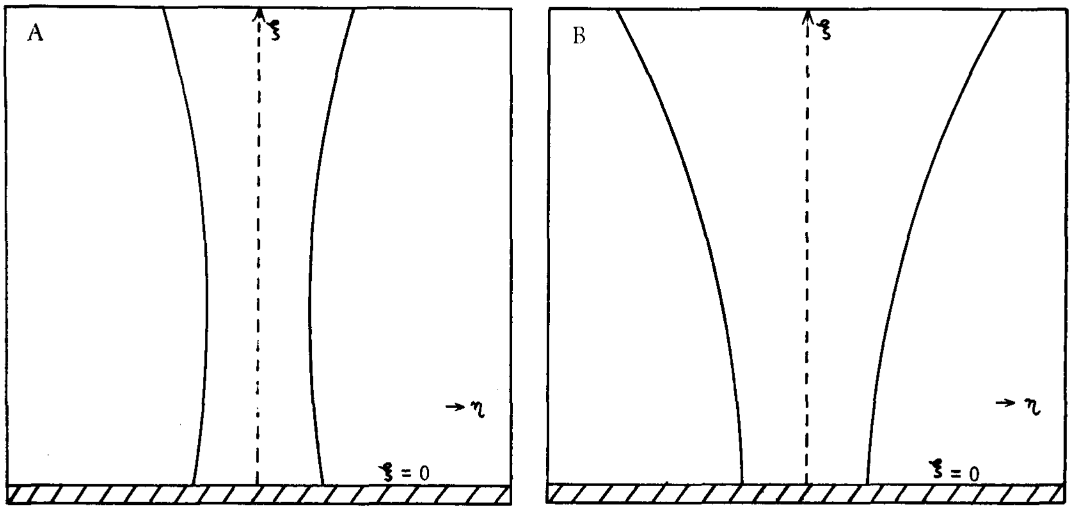

Fig. 9. Typical isobaric surfaces for *A*, a separated solution and *B*, an unseparated solution. Pressure decreases towards the ξ-axis.

shaped well away from the boundary. Furthermore, in the separated case, after initially converging as the ground is approached, they begin to diverge. If the hydrostatic background pressure field of the earth's atmosphere $p_0(z)$, say, is also included, the resulting actual isobars have qualitatively similar behaviour. In particular, for the separated solution, a broadening of the actual isobaric surfaces near the ground can occur, a feature which has been noted in many tornadoes.

6. Conclusions

It has been shown in the present work that the velocity field

$$u = \frac{r}{2t}F'(\xi) \qquad v = \frac{\Omega r}{4t}H(\xi) \qquad w = -2\sqrt{\frac{\nu}{t}}F(\xi)$$

where F, H satisfy

$$F''' + 2\xi F'' + 4F' + 4FF'' - 2(F')^2 + \frac{\Omega^2}{2}(H^2 - 1) = 2$$

$$H'' + 2\xi H' + 4H = -4(FH' - F'H)$$

subject to the boundary conditions

$$F(0) = F'(0) = H(0) = 0$$

$$F(\xi) \to \xi - C, \quad H(\xi) \to 1 \quad \text{as } \xi \to \infty$$

is an exact solution of the Navier–Stokes equations under the conditions stated at the beginning of section 2.

The results showed that for $0 \leqslant \Omega^2 \leqslant 4.952$, there exist boundary layer solutions for which radial flow is everywhere outward and the axial flow downward. For $\Omega^2 > 4.952$, however, there is a cell of reversed flow adjacent to the ground in which the opposite holds.

In considering the flow in a tornado vortex, this model has several inadequacies. Of particular importance is the failure to satisfy the condition that the velocities tend to zero as $r, z \to \infty$. Effects of turbulence are not included although it is likely that in the region where such a solution may be relevant, i.e. in the solid rotating central core, the flow is lightly stressed, and such effects are not important. Compressibility and buoyancy forces are also neglected. This is not completely justified, but it can be argued that the magnitudes of the velocities suggested in a tornado are neither so large that compressibility effects will be important nor so small as to give buoyancy forces time to become significant. A more fundamental weakness is that the simple time-dependence inherent in this work cannot successfully model the considerably more complicated time development of a tornado vortex. For example, the present model has a singularity in the velocity field at $t = 0$. However, in the formative stage of a tornado, the relevance of the model is in considerable doubt anyway as a basic requirement, namely the solid rotating central core for all ξ, is not fulfilled. (Observations tend to suggest that the disturbance grows down from the cloud structure during formation.) With these considerations in mind and noting from (24) that the circulation decreases with time, the relevance of the model is limited to the viscous decay stage of a tornado core.

In spite of these inadequacies, the solution does allow the no-slip condition to be satisfied and it also models the viscous effects in an established central core by assuming a solid body rotation. It also suggests the possibility of unifying the two types of tornado core flow discussed in the introduction in terms of the angular momentum in the central regions of the core.

Finally, it should be noted that the angular velocity in this core model is $\Omega/4t$ and not just Ω. Therefore low values of Ω^2 (i.e. $< A$) do not necessarily correspond to low angular velocities and similarly, high values of Ω^2 (i.e. $> A$) do not necessarily imply high angular velocities.

It is hoped that, in spite of its limitations, this model may help to throw some light on this extremely complicated problem.

Acknowledgements

The author is deeply indebted to Dr P. G. Bellamy-Knights for many helpful discussions and also to Dr I. M. Hall for his advice. This work was prepared during the tenure of a Research Studentship provided by the Science Research Council.

REFERENCES

Bellamy-Knights, P. G. 1970. An unsteady 2-cell vortex solution of the Navier–Stokes equations. *J.F.M. 41*, 673.

Bellamy-Knights, P. G. 1971. Unsteady multicellular viscous vortices. *J.F.M. 50*, 1.

Bellamy-Knights, P. G. 1974. An axisymmetric boundary layer solution for an unsteady vortex above a plane. Tellus *26*, 318.

Burgers, J. M., 1940. Application of a model system to illustrate some points of the statistical theory of free turbulence. *Proc. Acad. Sci. Amst. 43*, 2–12.

Burgers, J. M. 1948. A mathematical model illustrating the theory of turbulence. *Adv. Appl. Mech. 1*, 197–199.

Gutman, C. N. 1957. Theoretical model of a waterspout. *Bull. Acad. Sci. U.S.S.R.* (Geophysics series) *1*, 79.

Hoecker, W. H. 1960. Wind speed and airflow patterns in the Dallas tornado of 2nd April 1957. *Monthly Weather Review 88*, 167.

Morton, B. R. 1972. Private communication.

Oseen, C. W. 1911. *Ark. Mat. Astr. Fys. 7.*

Rossman, F. O. 1960. On the physics of tornadoes. *Cumulus dynamics*, p. 167. Pergamon Press, Oxford.

Rott, N. 1958. On the viscous core of a line vortex. *Z. Angew. Math. Phys. 9b*, 543–553.

Rott, N. 1959. On the viscous core of a line vortex II. *Z. Angew. Math. Phys. 10*, 73–81.

Serrin, J. 1972. The swirling vortex. *Phil. Trans. Roy. Soc. A. 271*, 325–360.

Sullivan, R. D. 1959. A 2-cell solution of the Navier–Stokes equations. *J. Aerospace Sci. 26*, 767.

Ward, N. B. 1972. The exploration of certain features of tornado dynamics using a laboratory model. *J. Atmos. Sci. 29*, 1194–1204.

ТЕЧЕНИЕ В СЕРДЦЕВИНЕ ВИХРЯ ВБЛИЗИ ТОЧКИ ЗАСТОЯ

В осесимметричном вихре, соприкасающемся с плоской границей, перпендикулярной оси симметрии, вязкие эффекты будут существенны в сердцевине вихря и вблизи границы. Некоторые модели сердцевины вихря изучались Роттом (1958, 1959) и Беллами–Найтсом (1970, 1971) в пренебрежении эффектами вблизи границы. Область пограничного слоя вдали от оси симметрии изучалась Беллами–Найтсом (1974). На границе и вблизи оси симметрии эти две вязких области будут взаимодействовать. Данная статья имеет целью объединить течения, изучавшиеся Беллами–Найтсом (1971, 1974), путем вывода уравнений подобия, справедливых в этой области взаимодействия, которые переходят асимптотически в уравнения пограничного слоя при возрастании радиуса и стремятся к уравнениям, описывающим сердцевину, с ростом расстояния от границы. Точное решение нестационарных вязких осесимметричных уравнений Навье–Стокса для несжимаемой жидкости, соответствующих сердцевине и области взаимодействия, на-

ходится в качестве частного случая решения общих уравнений путем использования метода разделения переменных. Уравнения Навье–Стокса сводятся к двум сцепленным обыкновенным дифференциальным уравнениям, которые решаются численно. Решения могут быть использованы для моделирования условий, существующих в центре вихря типа торнадо. Имеются расхождения по вопросу о направлении вращения в таких вихрях, так как существуют доказательства возможности обоих направлений вращения. Описанные здесь решения обладают интересным свойством: каждое из них возможно в зависимости от величины Ω-параметра, пропорционального угловой скорости вне пограничного слоя. Кроме того, при некоторых обстоятельствах можно предположить существование наверху точки застоя на оси вихря.